

# Path Integral Monte Carlo Simulations of Nanowires and Quantum Point Contacts <sup>1</sup>

**J. Shumway**

Department of Physics and Astronomy  
Arizona State University, Tempe AZ 85287-1504

**M. J. Gilbert**

Department of Electrical Engineering and Center for Solid State Electronics Research  
Arizona State University, Tempe, Arizona 85287-5706,  
Microelectronics Research Center, University of Texas, Austin, Texas 78758

**Abstract.** We study quantum wires and point contacts with a fixed-node path integral Monte Carlo technique. The fixed-node technique uses a variational principle to map fermionic problems into effective bosonic problems, which are then evaluated with standard quantum Monte Carlo techniques. While fixed-node is an approximation, it has the useful properties of being variational and being able to recover the exact answer when the exact nodes or phases of the density matrix are known. In these finite-temperature simulations we use the free-particle density matrix as a fixed-node constraint to efficiently simulate hundreds of interacting electrons. We have calculated charge densities, pair correlation functions, and the current-current Matsubara Green's functions for quantum wires and quantum point contacts.

## 1. Introduction

Nanostructures provide unique opportunities to engineer the properties of interacting electrons. Transport in such systems is sensitive to the dimensionality, shape, and size of the electron-confining regions. Temperature can also play a significant role, since quantum mechanics establishes energy scales that are often similar to the device operating temperatures. In this paper we describe a new method for simulating interacting electrons in semiconductor nanostructures at finite temperature.

Our approach is suitable for electrons in thermal equilibrium. While thermal equilibrium may seem uninteresting for devices, in fact, the thermal and quantum fluctuations in the equilibrium ensemble provide insight into transport through linear response theory. We focus on low-bias direct-current (DC) conductivity, for which sufficient numbers of interesting problems exist to justify development of new nanoscale simulation techniques.

We start from the Feynman path integral expression for the  $N$ -electron thermal density matrix [1],

$$\rho(R, R'; \beta) = \frac{1}{N!} \sum_P (-1)^P \int \mathcal{D}R(\tau) \exp(-S[R(\tau)]) \quad (1)$$

<sup>1</sup> Based on a talk presented at the conference "Progress in Nonequilibrium Green Functions III, Kiel, Germany, 22. – 25. August 2005"

where  $R = (\mathbf{r}_1, \dots, \mathbf{r}_N)$  are the particle coordinates, and the paths begin at  $R(0) = R'$  and end at  $R(\beta) = PR$ . The “imaginary time,”  $\tau$ , runs over an interval  $\beta = 1/k_B T$  and encodes the simulation temperature (we take  $\hbar = 1$ ). To handle spin, we work in a fixed  $S_Z$  ensemble, and restrict our permutation sum  $\sum'_P$  to only include permutations among the first  $N_\uparrow$  electrons and among the last  $N_\downarrow$ . Permutations that swap particles with differing spin states are not allowed in the ensemble. This fixed- $S_z$  ensemble is unphysical, but is a reasonable approximation if the number of electrons is large. For example, an unpolarized system has  $S_z = 0$ , and by fixing  $N_\uparrow = N_\downarrow = N/2$  we are just neglecting fluctuations in  $S_z$ , which become unimportant for large  $N$  (we have  $N \gtrsim 100$ ).

The action occurring in Eq. (1) is the imaginary time, or Euclidean, action, which resembles the classical energy,

$$S[R(\tau)] = \int_0^\beta \left( \frac{1}{2} m^* \left| \frac{dR(\tau)}{dt} \right|^2 + V(R(\tau)) \right) d\tau. \quad (2)$$

The potential energy includes pairwise coulomb interactions between electrons and the interaction of the electrons with an external confining potential,

$$V(R) = \sum_{i < j} \frac{e^2}{\epsilon r_{ij}} + \sum_{i=1}^N V_{\text{ext}}(\mathbf{r}_i). \quad (3)$$

In this paper we report on results for two-dimensional models in quantum dots, but we can also use more complicated three-dimensional potentials for  $V_{\text{ext}}(\mathbf{r})$ , including strained band offsets and the full Poisson solution for electrostatic gates.

One can discretize the paths and use Metropolis Monte Carlo integration to directly sample the density matrix of Eq. (1). Unlike classical statistical mechanics, for which Boltzmann factors,  $\exp(-\beta\epsilon)$ , are always positive, the expression for the Fermion density matrix has negative terms. Taken literally, Eq. (1) tells us to simulate a system of bosons, then use the negative signs to project out the properties of fermions from the antisymmetric fluctuations. As the number of particles gets large and the temperature gets low, this algorithm becomes exponentially inefficient, since a Bose condensate and a degenerate Fermi gas have very different physical properties. In a model of a quantum point contact, for example, bosonic electrons would condense outside the channel with essentially no quantum fluctuations into the channel, while Fermi pressure would force fermionic electrons into the channel. We must therefore make an approximation to have an efficient and practical algorithm for nanoscale electronics.

In this paper we give an overview of this new technique for path integral device simulations. In Sec. 2 we describe the fixed-node approximation for efficient path integral Monte Carlo (PIMC) simulations of fermions. In Sec. 3 we briefly discuss how to sample the fixed-node path integral using Monte Carlo integration. In Secs. 4 and 5 we explain how we estimate charge densities, correlation functions, and conductivity in PIMC. We present a demonstration calculation of two-hundred electrons around a quantum point contact in Sec. 6. Finally, in Sec. 7 we conclude with a summary and outlook for future PIMC simulations.

## 2. Fixed-node approximation for path integrals

Details of the fixed-node approximation are given in Ref. [2]. In this section we give an overview of the important features of the approximation. To make a fixed-node approximation, we first guess a form for the fermionic density matrix  $\rho_T(R, R'; \beta/2)$  corresponding to a temperature that is twice the simulation temperature. The fixed node approximation will sample the best

density matrix of the form [2],

$$\rho_f(R, R'; \beta) = \int f(R, R'') \rho_T(R, R'') \quad (4)$$

$$f(R'', R') \rho_T(R'', R') dR'', \quad (5)$$

where  $f$  is a positive-real envelope function with Bose symmetry. We demand that the envelope  $f$  maximizes the entropy of the density matrix, equivalent to minimizing the free energy. That is,

$$\frac{\delta}{\delta f} \{S[\rho_f] + \beta E[\rho_f] + \alpha N[\rho_f]\} = 0, \quad (6)$$

where the entropy is  $S[\rho_f] = -\text{tr} \rho_f \log \rho_f$ , the energy is  $E[\rho_f] = \text{tr} \hat{H} \rho_f$ , the normalization is  $N[\rho_f] = \text{tr} \rho_f$ , and there are two Lagrange multipliers,  $\alpha$  and  $\beta$ .

Evaluating Eq. (6) for the density matrix in Eq. (4) leads to an effective bosonic path integral with fixed-node action,[2]

$$S_{\text{FN}} = \begin{cases} 0; & \text{if } \rho_T(R(t), R(t + \beta/2)) \neq 0 \mid \forall t \in [0, \beta/2). \\ +\infty; & \text{otherwise.} \end{cases} \quad (7)$$

That is, we eliminate paths configurations that cross the nodes of  $\rho_T$  from the path integral. If the nodes of  $\rho_T$  exactly match the nodes of the the true density matrix of the interacting system, then the fixed node solution is exact, otherwise we get a density matrix with larger free energy. This fixed-node constraint is an approximate alternative to the explicit anti-symmetrization in Eq. (1). In a sense, the fixed-node path integral method is a sequence of two mappings. First we map the interacting fermions onto an effective interacting bosonic system with the fixed-node approximation. Then we use the path integral formalism to map the effective bosonic system to a classical statistical ensemble of paths which we can simulate with Metropolis Monte Carlo. This formulation of the fixed-node approximation, Eq. (7), has several useful features, especially relative to the fixed-node method of Ceperley [3]: (i) it keeps imaginary time symmetry in the paths, (ii) requires  $\rho_T$  only at  $t = \beta/2$ , (iii) can easily reach low temperature limit, (iv) has been proven to minimize the free energy, and (v) is easy to program and parallelize.

### 3. Path integral Monte Carlo

We use established techniques for the numerical evaluation of the path integral. An in-depth introduction to PIMC can be found in a review by Ceperley [4], and a review of our recent applications to semiconductors can be found in Ref. [5]. We work at a temperature of 3K, and discretize our path into  $M = 1000$  slices with a timestep of  $\Delta\tau = \beta/M$ . The interaction of the electrons with the external potential is treated with the primitive approximation [4],

$$S_{\text{ext}} = \sum_{j=1}^M \sum_{i=1}^N V_{\text{ext}}(\mathbf{r}_{i,j}) \Delta\tau, \quad (8)$$

where  $\tau = \beta/M$  and  $\mathbf{r}_{i,j}$  refers to position of particle  $i$  on discretized slice  $j$ . The kinetic contribution to the action is

$$S_{\text{kin}} = \sum_{j=1}^M \sum_{i=1}^N \frac{1}{2} m^* \frac{|\mathbf{r}_{i,j} - \mathbf{r}_{i,j-1}|^2}{(\Delta\tau)^2} \Delta\tau. \quad (9)$$

For the coulomb interactions, we must be more careful and use the pair-approximation, described in Ref. [4]. We have also partially screened the Coulomb interactions by including a metallic screening layer 100 nm below the device, using image charges.

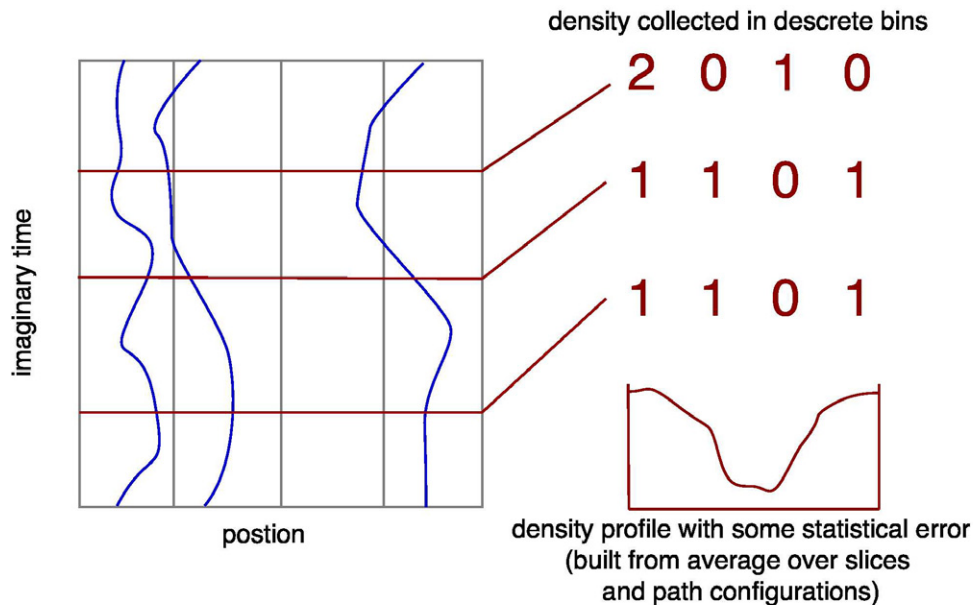


**Figure 1.** Schematic illustration of the collection of charge density information from a path integral simulation. We set up discrete real space bins (typical size  $10 \text{ nm} \times 10 \text{ nm}$  for a  $100 \times 50$  array), then histogram the location of discretized beads over many slices and path configurations.

To evaluate the path integral, we use multilevel Metropolis Monte Carlo to sample the path positions and permutations [4]. We use up to eight-levels of sampling, meaning that we reconstruct  $2^8 - 1 = 255$  slices of the path in one extended Monte Carlo step, moving one, two, or three particles at a time [4]. We sometimes run in parallel, in which case we make smaller moves but have multiple processors working on different segments of imaginary time. The simulations take a couple days on a 3GHz Intel processor, and for analysis of current-current correlation functions we have combined data collected from 8 parallel Monte Carlo simulations with different random number seeds (simulation cloning).

#### 4. Charge densities and correlation functions

Because we work in a real space basis, the collection of charge density data is very straight forward. As in classical simulations, we divide space into discrete cells (typically  $10 \text{ nm}$  square), then histogram the positions of the paths at many different time slices (Fig. 1). This quantity is the diagonal of the single particle density matrix, or the charge density.

For correlation functions, we follow exactly the same procedure, but only collect density data conditional on some criteria. For example, we may want to know the charge density of up and down electrons when there is a spin-up electron in the center of the channel. For each measurement and at each slice, we check to see if there is a spin-up electron within, say,  $10 \text{ nm}$  of the center of the channel. If such electron is present, we histogram the densities of the other electrons. If no up electron is in the center of the channel, we record zeros in all the bins. The collected quantity is then the two-particle reduced density matrix,  $\rho(\mathbf{r}, \mathbf{r}_2)$  with  $\mathbf{r}_2$  integrated over the area of the criteria region in the center of the channel, i.e. a circle of radius  $10 \text{ nm}$ .

#### 5. Estimating conductivity with PIMC

We collect the current-current correlation function,

$$\Pi(x, x'; in\Delta\tau) = \langle j_x(x; 0)j_x(x'; in\Delta\tau) \rangle_\beta. \quad (10)$$

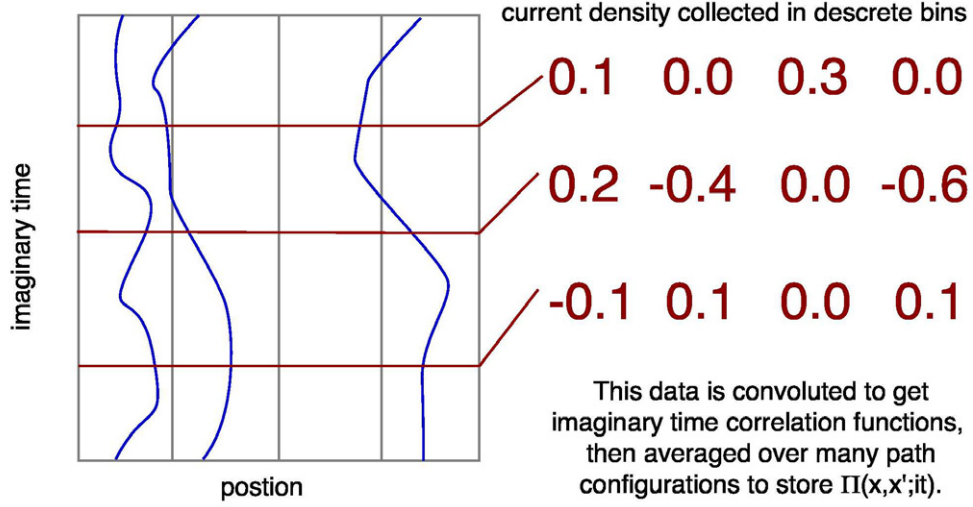


**Figure 2.** Schematic illustration of the collection of current charge density information from the path integral simulation. We set up discrete real space bins (typical size  $10 \text{ nm} \times 10 \text{ nm}$  for a  $100 \times 50$  array), then histogram the location and velocities of discretized beads at each slice over one path configuration. We then use an FFT to convolute the data for relative time separations, and collect  $\Pi(x, x'; i\tau)$  over many path configurations.

The Fourier transform is a set of real amplitudes at the bosonic Matsubara frequencies,  $\omega_n = 2n\pi/\beta$ ,

$$\Pi(x, x'; i\omega_n) = \sum_{m=0}^{M-1} \Delta\tau e^{i\omega_n m \Delta\tau} \Pi(x, x'; im\Delta\tau). \quad (11)$$

Note that the highest Matsubara frequency we can collect is  $\omega_M = \pi/\Delta\tau$ , our discretization of the path integral with timestep  $\tau$ . Of course, any physically relevant observable should have negligible contributions from large frequencies,  $\omega_n \gtrsim \pi/\tau$ , otherwise we need a smaller  $\Delta\tau$ .

The conductivity is given by the Kubo formula [6],

$$\sigma(x, x'; \omega) = \frac{i}{\omega} \left[ \Pi(x, x'; \omega) + \frac{ne^2}{m} \right]. \quad (12)$$

To obtain  $\Pi(x, x'; \omega)$  requires analytic continuation from the Matsubara frequencies, formally denoted  $i\omega_n \rightarrow \omega + i\delta$ . Of course, our simulations just collect real valued data, so this formal notation is not too helpful. The  $i\delta$  prescription means that for retarded Green's functions, the real frequency axis must be approached from upper half plane. In our simulations, the  $\omega = 0$  we have collected is the principle value, which is not the correct  $\omega \rightarrow 0_{+i}$  value for the Kubo formula. Instead, we must take the data collected for the Matsubara frequencies in the upper half plane and analytically continue them to small, real-valued frequencies.

## 6. Example: Two Hundred Interacting Electrons around a Quantum Point Contact

As an example, we describe preliminary calculations of 200 interacting electrons around a quantum point contact. A detailed study of quantum point contacts will require many calculations and careful tests, and is on-going. The results presented here only serve as an early demonstration of the techniques we have described.

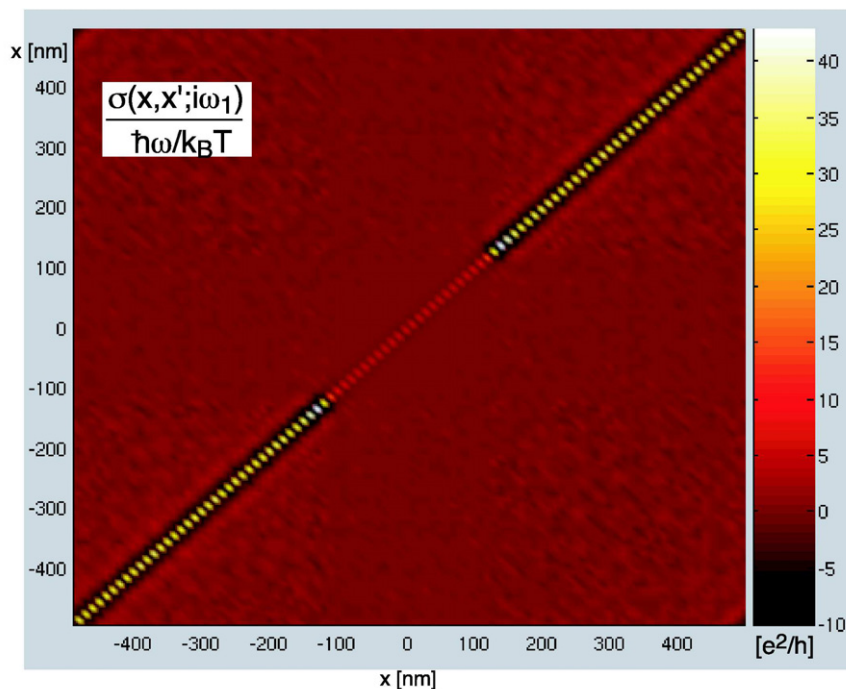


**Figure 3.** The conductivity at the first Matsubara frequency, as calculated by sampling the current-current correlation function for 200 interacting electrons in a PIMC simulation.

For our device model, we have taken an empirical expression for a double-gate barrier [7]. The device has a channel between the double-gates that is 200 nm long and 50 nm wide. The simulation is performed in a supercell that is  $1.0\mu\text{m}$  long and  $0.5\mu\text{m}$  wide. We place 200 electrons in the simulation, set the temperature to 3 K (1000 discretized slices), and run multilevel Metropolis sampling on the paths [4].

We have sampled the current-current correlation function,  $\Pi(x, x'; i\omega_n)$ , as described in Sec. 5. In Fig. 3 we show the conductivity at the first Matsubara frequency. We note that it is essentially diagonal, and the conductivity is suppressed within the channel. To calculate conductance, we must solve for the steady-state current in the  $\omega \rightarrow 0_{+i}$  limit. This requires analytic continuation of the conductivity from the upper half plane. At this time, we have attempted several different analytic continuation procedures, including N-point Padé expansions. We have found that the results have varied depending on our procedure, especially the number of Matsubara frequencies we include in our extrapolation. Since we do not have a clear estimate of our errors, and do not have enough simulations to show trends in the conductance versus gate voltages, we will not report our values here. We hope to present a clear analysis of the analytic continuation of our results to DC conductance in the very near future.

## 7. Outlook and future directions

This is a very new project, with initial test calculations on much smaller quantum wires first conducted less than six months ago. At this point, the technique appears quite promising. The simulations of two hundred electrons at  $T = 3\text{K}$  indicate that the method is practical for many current problems in nanoscale device modeling. While we do not have reliable conductance estimates yet, we think that the DC conductivity should be quite tractable. Of particular

interest would be the calculation of quantized conduction steps as a function of gate voltage [8], which is usually obtained more directly through the Landauer-Büttiker formalism [9, 10] .

One current problem this method may be able to approach is the so-called “0.7 structure,” which is a small bump in the conductance right before the first conductance plateau [12, 13]. Since PIMC can simulate interacting electrons at finite temperature, in a many-body formalism that correctly models exchange and correlation effects, it seems that we have the right ingredients for a quantitative simulation of this effect in a realistic device model.

Another area we would like to develop is the application of this technique to molecular conductors. Since path integrals have been useful in the determination of the polaron mass [14], PIMC might be a good framework for studying the effects of thermal vibrations and other distortions of molecules on their electrical conductivity. Such simulations would be analogous to the semiconductor simulations presented here, only the two-dimensional electron gas would be replaced by jellium, and the channel would be a molecule. Some preliminary results for PIMC calculations on small molecules and atoms are presented in Refs. [15] and [16].

This work supported by the National Science Foundation under Grant No. DMR 0239819 and computer resources from the Fulton High Performance Computing Initiative of Arizona State University.

- [1] R. P. Feynman. *Statistical Mechanics*. Addison-Wesley, Reading, MA, 1972.
- [2] Daejin Shin and J. Shumway. Fixed phase and fixed-node approximation for fermionic path integrals. in preparation, 2006.
- [3] D. M. Ceperley. *Phys. Rev. Lett.*, 69:331–334, 1992.
- [4] D. M. Ceperley. *Rev. Mod. Phys.*, 67:279–355, 1995.
- [5] M. Harowitz, Daejin Shin, and J. Shumway. *J. of Low Temp. Phys.*, 140:211–226, 2005.
- [6] R. Kubo. In W. E. Brittin and L. G. Dunham, editors, *Some Aspects of the Statistical-Mechanical Theory of Irreversible Processes*, Lectures In Theoretical Physics Vol. 1. Interscience, New York, 1959.
- [7] Gregory Timp. *Semiconductors and Semimetals*, 35:113–190, 1992.
- [8] L. P. Kouwenhoven, B. J. van Wees, C. J. P. M. Harmans, J. G. Williamson, H. van Houten, C. W. J. Beenakker, C. T. Foxon, and J. J. Harris. *Phys. Rev. Lett.*, 39:8040–8043, 1989.
- [9] R. Landauer. *IBM J. Res. Dev.*, 1:233, 1957.
- [10] M. Büttiker, Y. Imry, R. Landauer, and S. Pinhas. *Phys. Rev. B*, 31:6207, 1985.
- [11] N. K. Patel, J. T. Nicholls, L. Martn-Moreno, M. Pepper, J. E. F. Frost, D. A. Ritchie, and G. A. C. Jones. *Phys. Rev. B*, 44:13549–13555, 1991.
- [12] K. J. Thomas, J. T. Nicholls, M. Y. Simmons, M. Pepper, D. R. Mace, and D. A. Ritchie. *Phys. Rev. Lett.*, 77:135–138, 1996.
- [13] Kenji Hirose, Yigal Meir, and Ned S. Wingreen. *Phys. Rev. Lett.*, 90:026804, 2003.
- [14] R. P. Feynman and A. R. Hibbs. *Quantum Mechanics and Path Integrals*. McGraw-Hill, New York, 1965.
- [15] J. Shumway. All-electron path integral Monte Carlo simulations of small atoms and molecules. In D. P. Landau, S. P. Lewis, and H. B. Schüter, editors, *Computer Simulations Studies in Condensed Matter Physics XVII*, pages 181–195. Springer Verlag, Heidelberg, Berlin, 2006.
- [16] Daejin Shin, Ming-Chak Ho, and J. Shumway. Ab-initio path integral techniques for molecules. in preparation, 2006.